

# A robust super twisting fractional-order sliding mode-based control of vehicle longitudinal dynamic subjected to a constant actuator fault

Imane Abzi, Mohammed Nabil Kabbaj, Mohammed Benbrahim

Department of Engineering, Modeling and Systems Analysis Laboratory (LIMAS), Faculty of Sciences Dhar El Mahraz, Sidi Mohamed Ben Abdellah University, Fez, Morocco

## Article Info

### Article history:

Received Jul 1, 2021

Revised May 22, 2023

Accepted Jun 4, 2023

### Keywords:

Fractional order

Longitudinal dynamic

Robust

Sliding mode control

Super twisting

## ABSTRACT

This paper deals with the design and analysis of a super twisting fractional-order sliding mode controller (ST-FOSMC) to adjust the vehicle longitudinal dynamic when braking. While vehicle loading, road types, and modeling uncertainties are time-varying parameters, the control law must be robust against these disturbances. Also, the aging of the brake plate may introduce a difference between the control output and the actuator response that should be considered. The proposed control strategy has been used to enable the anti-lock braking system (ABS) to track the desired wheel slip value despite the presence of disturbances and constant actuator fault. The design of this controller is presented and the system stability is guaranteed by applying the Lyapunov theory. We carried out a simulation example that makes a comparison between our controller and the one based on the fractional-order sliding mode control to investigate which one of them outperforms the other. The results exhibit the superiority of the super twisting fractional order controller over the traditional fractional-order sliding mode controller during the braking phase.

*This is an open access article under the [CC BY-SA](https://creativecommons.org/licenses/by-sa/4.0/) license.*



## Corresponding Author:

Imane Abzi

Department of Engineering, Modeling and Systems Analysis Laboratory (LIMAS), Faculty of Sciences Dhar El Mahraz, Sidi Mohamed Ben Abdellah University

Fez, 30000, Morocco

Email: imane.abzi@usmba.ac.ma

## 1. INTRODUCTION

Recent advancements in embedded systems have led to noticeable progress in the electronic control of vehicle dynamics. Therefore, this achievement makes the active safety systems carry out a vital role to protect the life of vehicle passengers. One of the most important active safety systems is the anti-lock braking system (ABS), which controls the wheel slip to prevent the risk of locking up a wheel in emergency situation and critical braking. When the sensors located in each wheel detect an over-slip, the computer alleviates the brake pressure on this wheel.

Several researches in the literature have addressed the control of the wheel slip [1]. The vehicle will likely slide after severe braking or slippery road condition, especially icy surfaces. Consequently, the car will lose its lateral stability, and the braking distances will increase. Therefore, the purpose of the ABS consists of the control and adjustment of the wheel slip. In other words, it aimed to track the predefined value, along with keeping the tire adhesion at its maximum.

During the braking phase, the adhesion between the vehicle's wheel and the road surface produces the tractive forces  $F_x$  that are expressed as the product of the road coefficient of adhesion  $\mu$  and the vertical

forces  $F_z$ . Several studies have proven that  $\mu$  can be expressed as a mathematical function of the wheel slip  $\lambda$ . Figure 1 depicts the curves of  $\mu$  against  $\lambda$  in various road types.  $\lambda$  varies between 0 and 1. According to Figure 1, one can observe that whenever the road surface has been more slippery, the friction becomes very weak, which will influence the vehicle stability. It is noticed that the value 0.2 of the wheel slip has a good friction coefficient for all surfaces. Owing to the mentioned analysis, the main object of designing ABS is maintaining the slip ratio  $\lambda$  as near as possible to the reference value 0.2, in which the active force reaches its maximum value. Thus, the braking is efficient (which cannot be attained when the desired slip is zero).

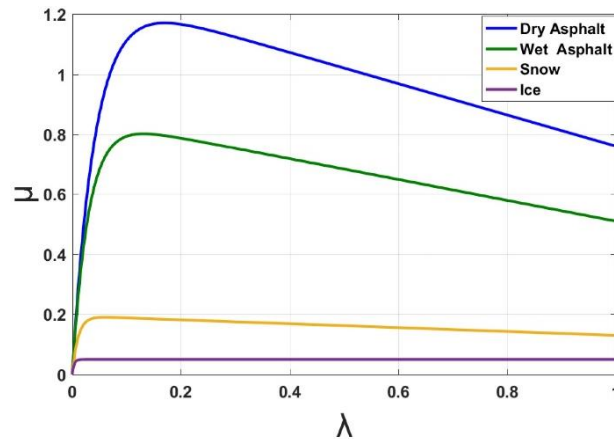


Figure 1. Friction coefficient versus wheel slip for various road types

In recent decades, the control of nonlinear systems has been one of the most challenging areas in the field of control theory. Various control techniques have been innovated and successfully integrated for better performance and accuracy in closed-loop for many classes of nonlinear systems [2], [3]. Among the proposed methods, the sliding mode control (SMC) aroused great interest due to its flexibility and robustness [4], [5]. Therefore, it has been widely applied to design ABS controllers. Chaudhari *et al.* [6] propose a disturbance observer combined with the SMC approach for ABS, which aimed to compensate model parameters variation. A time-varying SMC strategy for the control of the longitudinal dynamics of an electric car has been presented and compared with experimental results [7]. In parallel, some research works have built up fuzzy adaptive [8] neuro-adaptive [9] and SMC that estimate accurately the uncertainties and external disturbances. A new digital SMC technique has been elaborated in [10] to tackle the issue of integration of ABS controllers in electronic boards. Also, an improved conventional SMC for wheel slip control has been developed in the literature [11].

The main drawback of the SMC based strategies is the chattering effect. This undesirable phenomenon reduces the lifetime of the ABS mechanical parts and impacts the control accuracy. Many solutions have been proposed to overcome these issues [12], [13]. One of them consists in utilizing a higher-order SMC as described in [13]. However, further improvements are needed to suppress this harmful effect.

The previously mentioned techniques and strategies belong to the category of classical SMC. That means the order of integration or derivation in the sliding surface is always an integer. After its emergence more than three-century ago, the fractional calculus has known a spectacular development. But, its application in physics and engineering has been introduced only in the last few decades. While fractional derivatives and integrals are an extension to the natural ones, the fractional-order sliding mode controller (FOSMC), founded on this new mathematical paradigm, is similarly an extension of the conventional SMC.

The FOSMC has been adopted in many nonlinear systems such as autonomous vehicle [14], robot manipulators [15], DC-DC converters [16] and doubly-fed induction generator (DFIG) [17]. It should be emphasized that great efforts have been made to design FOSMC based ABS controllers [18]. For example, in [19], a FOSMC methodology that deals with the ABS control have been developed using the quarter-vehicle model. Furthermore, another FOSMC scheme based on a fuzzy adaptive controller has been used to mitigate the effect of disturbances [20]. More recently, an adaptive design of FOSMC controller that utilizes a fast terminal fractional-order sliding surface has been elaborated [21]. This large number of studies that have addressed FOSMC show its importance. To the best knowledge of the authors, there are no previous articles that have addressed the case when actuator faults arise. For this reason, the main objective of this paper is the design of a new controller based on the super twisting fractional-order sliding mode control that ensures the stability and high performances of the ABS under disturbances and constant actuator faults.

The rest of this paper is structured as follows: section 2 describes the chosen ABS modeling strategy. While section 3, deals with the design of FOSMC and ST-FOSMC controllers. Comparison of simulation results of both controllers is detailed in section 4. Finally, some conclusions and perspectives are drawn in section 5.

## 2. THE ABS SYSTEM MODELING

Modeling vehicle dynamics is a complex process. Each model developed in the literature is suitable for certain situations and shows its limits in others. When we study only the vehicle longitudinal dynamics under braking conditions, the quarter-vehicle model [19] is a good compromise between simplicity and results reliability. By applying Newton's law to the system described in Figure 2, the (1) and (2) are obtained.

$$m\dot{v} = -F_x \quad (1)$$

$$J\dot{\omega} = -T_b + rF_x \quad (2)$$

where  $T_b$  is the braking torque of control,  $F_x$  indicates the longitudinal friction force,  $\omega$  designates the angular speed of the wheel,  $r$  represents the wheel radius,  $J$  is the wheel inertia,  $m$  denotes the mass of the quarter vehicle and  $v$  is the vehicle longitudinal speed. According to Coulomb law,  $F_x$  can be expressed as (3).

$$F_x = \mu(\lambda)F_z \quad (3)$$

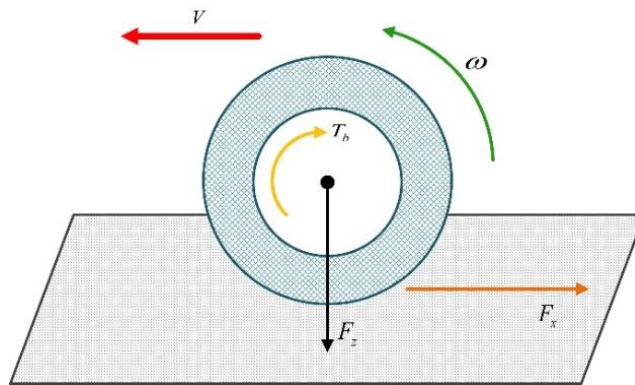


Figure 2. The quarter vehicle model under study

For the sake of simplicity, we consider  $F_z = mg$  where  $g$  designates the constant of gravitational acceleration. The variable  $\lambda$  which is the wheel slip allows quantifying the gap between the vehicle and the wheel velocities when the driver presses on the brake pedal. It is defined as (4),

$$\lambda = \frac{v-r\omega}{v} \quad (4)$$

$\lambda$  is the state of interest in designing the ABS controller because only the slip ratio has a relationship to the road friction coefficient. This later, when it reaches its maximum, reduces the braking time. The wheel velocity cannot be greater than the vehicle velocity during the braking phase, for this reason,  $\lambda$  is always positive. By applying the time derivative to (4) and after substitution by (1) and (2) we can obtain the following general formula that is considered very useful to control the system:

$$\lambda = -\left(\frac{\dot{1}-\lambda}{mv} + \frac{r^2}{Jv}\right)\mu F_z + \frac{r}{Jv}T_b \quad (5)$$

In established studies, several models have been developed to model the friction force generated by the interaction between the vehicle tire and the road. There are those based on semi-empirical models like the Pacejka magic formula [22]. There are also physical models such as the Dugoff's tire model [11]. Meanwhile, the Burckhardt model [22] has been extensively used in controlling the vehicle longitudinal dynamics, owing to the simplicity of its formulation (6).

$$\mu(\lambda) = c_1(1 - e^{-c_2\lambda}) - c_3\lambda \quad (6)$$

with  $c_1$ ,  $c_2$ , and  $c_3$  are real coefficients that must be determined for each road type [23].

### 3. SMC, FOSMC AND ST-FOSMC ABS CONTROLLERS DESIGN

In this section, three controllers are proposed for the ABS. They are based on the longitudinal model in (5). Figure 3 depicts the control scheme of the system in a closed-loop. While the goal of these controllers consists in tracking the predefined slip ratio, let us define the following error of tracking (7),

$$e = \lambda - \lambda_d \quad (7)$$

where  $\lambda_d$  designates the reference slip ratio.

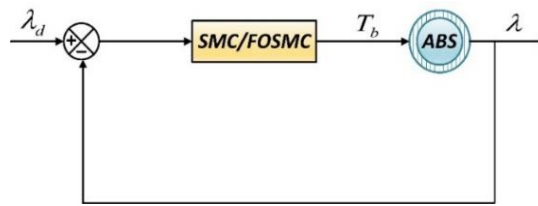


Figure 3. Control scheme

#### 3.1. SMC controller design technique for ABS

In designing SMC controllers, the first step is the choice of a suitable sliding surface. In recent research works, many types of sliding surfaces have been proposed and applied in the design stage [24], [25]. In our work, the following sliding surface is selected (8).

$$S_1 = k_1 e + \int e dt \quad (8)$$

where  $k_1$  denotes a positive constant.

The following control torque is considered (9).

$$T_b = T_{eq} + T_r \quad (9)$$

where  $T_{eq}$  represents the equivalent control. It is calculated under the constraint  $\dot{S}_1 = 0$ . While  $T_r$  is the robust nonlinear term that is used to compensate the unknown uncertainties. As shown in (10) and (11) explicit their expressions.

$$T_{eq} = \frac{Jv}{r} \left( -\frac{e}{k_1} + \frac{\mu F_z}{v} \left( \frac{1-\lambda}{m} + \frac{r^2}{J} \right) \right) \quad (10)$$

$$T_r = \frac{Jv}{r} k_2 \text{Sgn}(S_1) \quad (11)$$

where  $k_2$  is a real positive coefficient, and the sign function is defined as follows:

$$\text{Sgn}(S) = \begin{cases} +1, & \text{if } S > 0 \\ 0, & \text{if } S = 0 \\ -1, & \text{for } S < 0 \end{cases}$$

**Theorem 1.** Let us consider the nonlinear state model in (5) which is controlled by the control law given (9), (10), and (11), then, the dynamic of the wheel slip will coincide with the selected sliding surface (8).

*Proof.* Considering the following Lyapunov candidate function as in [19].

$$V_1 = |S_1| \quad (12)$$

Time derivative is applied to both sides of (12).

$$\dot{V}_1 = \dot{S}_1 \text{Sgn}(S_1) \quad (13)$$

The application of the time derivative on the sliding surface gives (14).

$$\dot{S}_1 = -k_1 k_2 \text{Sgn}(S_1) \quad (14)$$

After simplification of (14), one can obtain (15).

$$\dot{V}_1 = -k_1 k_2 |S_1| \quad (15)$$

The time derivative of  $V_1$  is negative. Thus, proving theorem 1.

### 3.2. FOSMC controller design technique

Before we proceed to the design of the controller of this section, it is underlined that some preliminaries of the fractional calculus are required [18]. Let us introduce the theorem that reveals the stability condition of an autonomous fractional-order system described by (16). It will help us to assess the stability of the fractional sliding surface.

$${}_0 D_t^\alpha x = Ax \text{ and } x(0) = x_0 \quad (16)$$

where  $\alpha$  designates the order of differentiation,  $A \in \mathbb{R}^{n \times n}$  and  $x \in \mathbb{R}^n$ .

Theorem 2. The system presented in (16) is asymptotically stable if  $|\arg(\text{eig}(A))| > \alpha\pi/2$  [26]. If the aforementioned condition holds, then the state vector decay towards vector zero like  $t^{-\alpha}$ . In the case where  $|\arg(\text{eig}(A))| \geq \alpha\pi/2$ , then the stability is guaranteed if also, the geometric multiplicity of those particular eigenvalues that verify  $|\arg(\text{eig}(A))| = \alpha\pi/2$  is equal 1.

In addition, the stability zone of the fractional order system characterized by  $\alpha \in ]0, 1[$  is larger than that with either  $\alpha \in ]1, 2[$  or  $\alpha = 1$ . Let us opt for the choice of the sliding surface  $PD^\alpha$  defined by (17).

$$S_2 = D^\alpha e + k_3 e \quad (17)$$

If condition  $S_2=0$  is fulfilled, then (17) becomes (18).

$$D^\alpha e = -k_3 e \quad (18)$$

According to (18),  $A = -k_3$ . So,  $|\arg(\text{eig}(A))| = \pi$ . Typically,  $\alpha$  is selected in the interval  $]0, 1[$ . This is due to the larger stability in this region. While  $|\arg(\text{eig}(A))| > \alpha\pi/2$ , the sliding surface dynamic is asymptotically stable.

The next equation provides the first derivative of the  $PD^\alpha$  sliding surface:

$$\dot{S}_2 = D^{\alpha+1} e + k_3 \dot{e} \quad (19)$$

where  $k_3$  represents a positive constant. Similarly, to the previous subsection, the control law has the expression (20).

$$U = U_{eq} + U_r \quad (20)$$

Once again, the term  $U_{eq}$  can be deduced by considering the constraint  $\dot{S}_2 = 0$ . But the robust term  $U_r$  is designed in another way to guarantee the system stability. The below expressions make that clearer:

$$U_{eq} = \frac{Jv}{r} \left[ \frac{\mu g(1-\lambda)}{v} + \frac{\mu F_z r^2}{Jv} - \frac{D^{\alpha+1} e}{k_3} \right] \quad (21)$$

$$U_r = \frac{Jv}{r} k_4 \text{Sgn}(S_2) \quad (22)$$

Theorem 3. Considering the nonlinear state model in (5) which is controlled by the control law given in (20), (21) and (22), then, the dynamic of the wheel slip will coincide with the selected sliding surface (17).

*Proof.* We opt for the use of the following classical Lyapunov function:

$$V_2 = \frac{1}{2} S_2^2 \tag{23}$$

Now, by taking time derivative of (23) results in (24).

$$\dot{V}_2 = \dot{S}_2 S_2 \tag{24}$$

The next equation is derived from the previous one:

$$\dot{V}_2 = k_3 S_2 (-k_4 \text{Sgn}(S_2)) \tag{25}$$

After simplification:

$$\dot{V}_2 = -k_3 k_4 |S_2| \tag{26}$$

The function  $V_2$  is positive, and its time derivative in the above equation is negative. According to the Lyapunov theorem the stability of the system is guaranteed.

**3.3. ST-FOTSMC controller design method**

In reality, the slip (5) fails to represent truly the ABS. For the sake of accuracy, it is mandatory to consider the model uncertainties and lumped disturbances. Therefore, in this subsection, we consider the (27),

$$\dot{\lambda} = -\left(\frac{1-\lambda}{mv} + \frac{r^2}{Jv}\right) \mu F_z + \frac{r}{Jv} (T_b + f) + d \tag{27}$$

where  $d$  denotes the sum of uncertainties and disturbances, and  $f$  is the constant actuator fault, the following assumption is considered throughout the (28).

$$d \leq \rho |\sigma|^{1/2} \tag{28}$$

The control scheme adopted in this subsection is described in Figure 4.

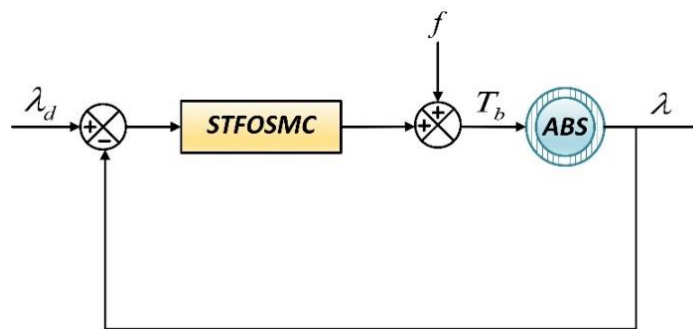


Figure 4. Control scheme with actuator fault

We use the same sliding surface  $PD^\alpha$  defined in the previous subsection (29).

$$\sigma = D^\alpha e + ce \tag{29}$$

where  $c$  is a positive real coefficient. The time derivative of (29) leads to:

$$\dot{\sigma} = D^{\alpha+1} e + c\dot{e} \tag{30}$$

The control torque can be written as (31).

$$T_b = T_{eq} + T_{sw} \quad (31)$$

So,  $T_b$  is the sum of the equivalent term  $T_{eq}$  that is derived from  $\dot{\sigma} = 0$ , and the super twisting term  $T_{sw}$ :

$$T_{eq} = \frac{Jv}{r} \left[ \frac{\mu g(1-\lambda)}{v} + \frac{\mu F_z r^2}{Jv} - \frac{D^{\alpha+1} e}{c} \right] - \hat{f} \quad (32)$$

$$T_{sw} = \frac{Jv}{cr} [-\gamma|\sigma|^{1/2} Sgn(\sigma) + \vartheta] \quad (33)$$

with:  $\dot{\vartheta} = -\beta Sgn(\sigma)$

Theorem 4. Considering the nonlinear state model including uncertainties and disturbances and actuator fault in (27) which is controlled by the super-twisting torque given in (31), (32) and (33), then, the dynamic of the system will pursue the predefined reference.

*Proof.* We define the Lyapunov function adopted to prove the stability of our system as (34).

$$V_3 = |\sigma| + \frac{1}{2\varepsilon} \vartheta^2 + \frac{1}{2\zeta} \tilde{f}^2 \quad (34)$$

The time derivative of the previous equation leads to the (35).

$$\dot{V}_3 = \dot{\sigma} Sgn(\sigma) + \frac{1}{\varepsilon} \dot{\vartheta} \vartheta + \frac{1}{\zeta} \dot{\tilde{f}} \tilde{f} \quad (35)$$

After simplification:

$$\dot{V}_3 = \left[ cd + c \frac{r}{Jv} \tilde{f} - \gamma |\sigma|^{1/2} Sgn(\sigma) + \vartheta \right] Sgn(\sigma) - \frac{1}{\varepsilon} \beta Sgn(\sigma) \vartheta - \frac{1}{\zeta} \dot{\tilde{f}} \tilde{f} \quad (36)$$

By choosing  $\varepsilon = \beta$  and considering the assumption in (28), the following holds:

$$\dot{V}_3 \leq (c\rho - \gamma) |\sigma|^{1/2} + \left( c \frac{r}{Jv} Sgn(\sigma) - \frac{1}{\zeta} \dot{\tilde{f}} \right) \tilde{f} \quad (37)$$

We choose  $\dot{\tilde{f}}$  and  $\gamma$  such that:  $\dot{\tilde{f}} = \frac{\zeta cr}{Jv} Sgn(\sigma)$  and  $\gamma > c\rho$ , After replacement in (37), the (38) is verified:

$$\dot{V}_3 < 0 \quad (38)$$

$\dot{V}_3$  is always negative. Thus, the system is stable.

#### 4. SIMULATION RESULTS

The purpose of the results section consists of comparing the response of the vehicle using the three controllers, through a simulation carried out under MATLAB Simulink. All tests are based on the dry asphalt road. Table 1 summarizes the vehicle parameters [21]. In the simulation scheme, the saturation function defined in (39) was used instead of the sign function in order to attenuate the phenomenon of chattering. Table 2 summarizes the three controllers parameters values.

$$sat\left(\frac{s}{\phi}\right) = \begin{cases} Sgn\left(\frac{s}{\phi}\right), & \left|\frac{s}{\phi}\right| \geq 1 \\ \frac{s}{\phi}, & \left|\frac{s}{\phi}\right| < 1 \end{cases} \quad (39)$$

Table 1. Vehicle's parameters

Parameters	Values
m	342 Kg
J	1.13 Kg.m <sup>2</sup>
g	9.8 m/s <sup>2</sup>
r	0.33 m
V	20 m/s

Table 2. The values of the controller's parameters

Parameters	Values	Parameters	Values
k <sub>1</sub>	40	k <sub>2</sub>	100
k <sub>3</sub>	15	k <sub>4</sub>	250
α	0.3	ϕ	2
c	1.2×10 <sup>3</sup>	β	1.8
γ	133×c	ζ	1×c

**4.1. Scenario 1: without actuator fault and model uncertainties**

In the first scenario, we ran a simulation under normal conditions without taking into account the model uncertainties and the actuator fault. The objective is to assess the response of the system under the three controllers by analyzing the slip ratio and braking distance. Based on Figure 5, it is shown that the ST-FOSMC and FOSMC controllers reach the desired slip ratio and follow it accurately. While the traditional SMC suffers from a lack of precision compared to the aforementioned controllers. Also, referring to Figure 6, the braking distance is the shortest when ST-FOSMC and FOSMC controllers are used.

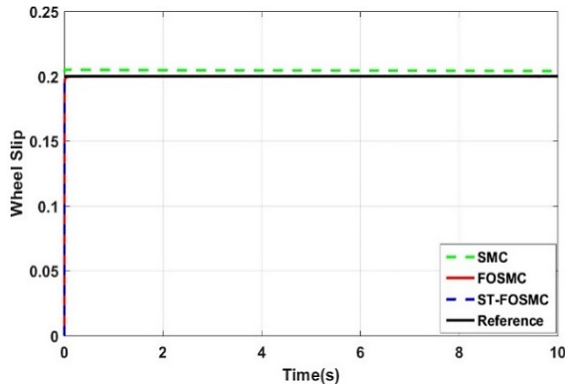


Figure 5. The wheel slip curves in the case of dry asphalt road

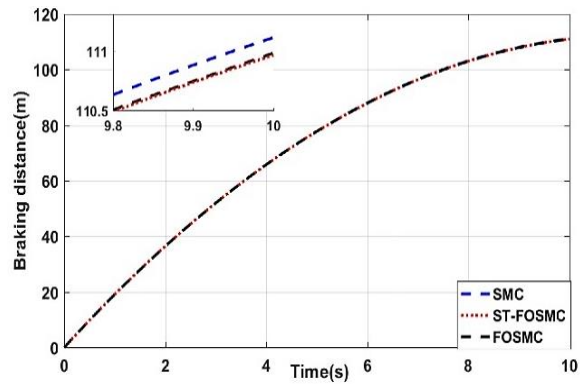


Figure 6. Braking distance of the first scenario

**4.2. Scenario 2: with model uncertainties:  $\Delta m = 50\% m$ ,  $\Delta r = 50\% r$ , and  $\Delta J = 50\% J$**

In this subsection, we have added the model uncertainties, such as the vehicle's mass variation, the wheel radius changes, and the wheel inertia uncertainties. As clearly shown in Figure 7, the vehicle loses its accuracy and starts to diverge after 8s when the SMC and FOSMC controllers are used. On the contrary, the vehicle keeps its stability and tracks accurately the desired slip ratio under the ST-FOSMC controller. In regards to the braking distance Figure 8, the ST-FOSMC controller offers the shortest distance. The FOSMC controller comes in the second position, while the SMC takes the third rank. That exhibits the importance of the ST-FOSMC controller in situations where the model uncertainties cannot be neglected.

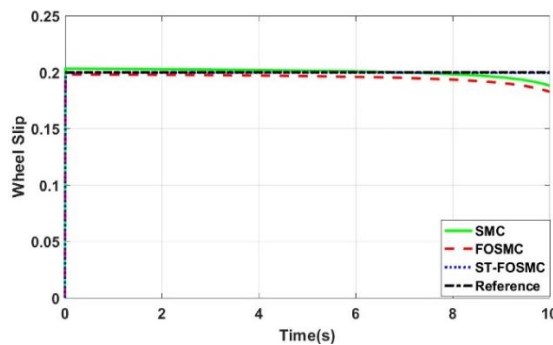


Figure 7. The wheel slip curves in the case of dry asphalt road

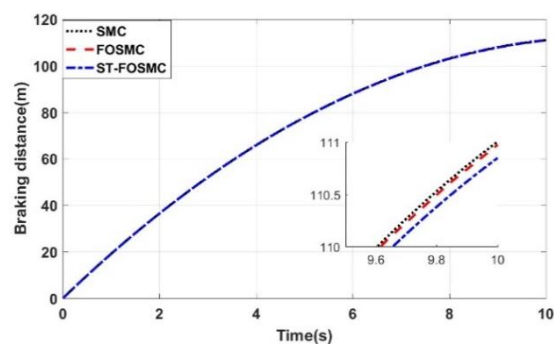


Figure 8. Braking distance of the second scenario

**4.3. Scenario 3: with actuator fault and model uncertainties:  $\Delta m = 50\% m$ ,  $\Delta r = 50\% r$ ,  $\Delta J = 50\% J$  and  $f = 50 N.m$**

In the last scenario, both the model uncertainties and the actuator fault are considered to evaluate the robustness of the controllers. Figure 9 depicts the performances of the three controllers. The SMC and the FOSMC controllers diverge and lose their stability after 8 s, while the ST-FOSMC demonstrates another time its high robustness and accuracy. Figure 10 shows that the braking distance of the ST-FOSMC controller is still the shortest when a constant actuator fault is added.



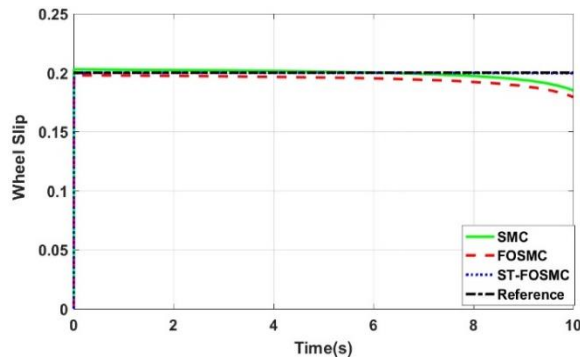


Figure 9. Time response of wheel slip for dry asphalt road

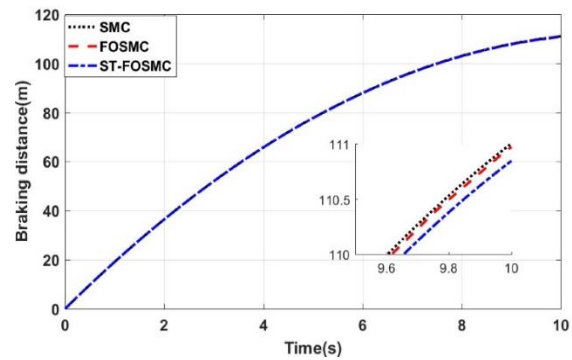


Figure 10. Braking distance of the third scenario

## 5. CONCLUSION

In this paper, we built up an ST-FOSMC controller for ABS considering constant actuator faults and external perturbations. The system stability has been ensured by satisfying the Lyapunov's theory. The results obtained by carrying out three simulations for different scenarios have demonstrated the effectiveness and the ability of the ST-FOSMC controller to maintain the system stability and performance under uncertainties and actuator fault. The advantages of our proposal are as follows: i) accurate and fast-tracking of the predefined reference value, ii) ensure the stability and nominal functioning under the occurrence of constant actuator faults and disturbances, and iii) the proposed controller design remains simple but efficient. Our future works may focus on the active fault-tolerant control of the ABS system under variable actuator fault, taking advantage of the performances of the fractional-order mathematical paradigm.




## REFERENCES

- [1] A. A. Aly, E.-S. Zeidan, A. Hamed, and F. Salem, "An antilock-braking systems (ABS) control: A technical review," *Intelligent Control and Automation*, vol. 02, no. 03, pp. 186–195, 2011, doi: 10.4236/ica.2011.23023.
- [2] I. Abzi, M. N. Kabbaj, and M. Benbrahim, "Fault tolerant control of vehicle lateral dynamic using a new Pneumatic force multiple model," *Actuators*, vol. 9, no. 4, Nov. 2020, doi: 10.3390/act9040120.
- [3] I. Abzi, M. N. Kabbaj, and M. Benbrahim, "Design of fractional order sliding mode controller for lateral dynamics of electric vehicles," in *ICEERE 2020: Proceedings of the 2nd International Conference on Electronic Engineering and Renewable Energy Systems*, 2021, pp. 573–581, doi: 10.1007/978-981-15-6259-4\_60.
- [4] S. Q. G. Haddad and H. A. R. Akkar, "Intelligent swarm algorithms for optimizing nonlinear sliding mode controller for robot manipulator," *International Journal of Electrical and Computer Engineering (IJECE)*, vol. 11, no. 5, pp. 3943–3955, Oct. 2021, doi: 10.11591/ijece.v11i5.pp3943-3955.
- [5] M. F. Zohra, B. Mokhtar, and M. Benyounes, "Sliding mode performance control applied to a DFIG system for a wind energy production," *International Journal of Electrical and Computer Engineering (IJECE)*, vol. 10, no. 6, pp. 6139–6152, Dec. 2020, doi: 10.11591/ijece.v10i6.pp6139-6152.
- [6] P. Chaudhari, V. Sharma, P. D. Shendge, and S. B. Phadke, "Disturbance observer based sliding mode control for anti-lock braking system," in *2016 IEEE 1st International Conference on Power Electronics, Intelligent Control and Energy Systems (ICPEICES)*, Jul. 2016, pp. 1–5, doi: 10.1109/ICPEICES.2016.7853488.
- [7] S. Rajendran, S. Spurgeon, G. Tsampardoukas, and R. Hampson, "Time-varying sliding mode control for ABS control of an electric car," *IFAC-PapersOnLine*, vol. 50, no. 1, pp. 8490–8495, Jul. 2017, doi: 10.1016/j.ifacol.2017.08.823.
- [8] B. K. Dash and B. Subudhi, "A fuzzy adaptive sliding mode slip ratio controller of a HEV," in *2013 IEEE International Conference on Fuzzy Systems (FUZZ-IEEE)*, Jul. 2013, pp. 1–8, doi: 10.1109/FUZZ-IEEE.2013.6622325.
- [9] C. Rosales, J. Gimenez, F. Rossomando, C. Soria, M. Sarcinelli-Filho, and R. Carelli, "UAVs formation control with dynamic compensation using neuro adaptive SMC," in *2019 International Conference on Unmanned Aircraft Systems (ICUAS)*, Jun. 2019, pp. 93–99, doi: 10.1109/ICUAS.2019.8798282.
- [10] D. B. Mitić, S. L. Perić, D. S. Antić, Z. D. Jovanović, M. T. Milojković, and S. S. Nikolić, "Digital sliding mode control of anti-lock braking system," *Advances in Electrical and Computer Engineering*, vol. 13, no. 1, pp. 33–40, 2013, doi: 10.4316/AECE.2013.01006.
- [11] N. Patra and K. Datta, "Sliding mode controller for wheel-slip control of anti-lock braking system," in *2012 IEEE International Conference on Advanced Communication Control and Computing Technologies (ICACCCT)*, Aug. 2012, pp. 385–391, doi: 10.1109/ICACCCT.2012.6320808.
- [12] H. U. Suleiman, M. B. Murazu, T. A. Zarma, A. T. Salawudeen, S. Thomas, and A. A. Galadima, "Methods of chattering reduction in sliding mode control: A case study of ball and plate system," in *2018 IEEE 7th International Conference on Adaptive Science & Technology (ICAST)*, Aug. 2018, pp. 1–8, doi: 10.1109/ICASTECH.2018.8506783.
- [13] S. Mondal and C. Mahanta, "Second order sliding mode controller for twin rotor MIMO system," in *2011 Annual IEEE India Conference*, Dec. 2011, pp. 1–5, doi: 10.1109/INDCON.2011.6139561.
- [14] K. Orman, K. Can, A. Basci, and A. Derdiyok, "An adaptive-fuzzy fractional-order sliding mode controller design for an unmanned vehicle," *Elektronika ir Elektrotechnika*, vol. 24, no. 2, pp. 12–17, Apr. 2018, doi: 10.5755/j01.eie.24.2.20630.
- [15] Y. Wang, J. Chen, F. Yan, K. Zhu, and B. Chen, "Adaptive super-twisting fractional-order nonsingular terminal sliding mode control of cable-driven manipulators," *ISA Transactions*, vol. 86, pp. 163–180, Mar. 2019, doi: 10.1016/j.isatra.2018.11.009.




- [16] N. Chafekar, U. M. Mate, S. R. Kurode, and V. A. Vyawahare, "Design and implementation of fractional order sliding mode controller for DC-DC buck converter," in *2019 Fifth Indian Control Conference (ICC)*, Jan. 2019, pp. 201–206, doi: 10.1109/INDIANCC.2019.8715589.
- [17] S. Ebrahimkhani, "Robust fractional order sliding mode control of doubly-fed induction generator (DFIG)-based wind turbines," *ISA Transactions*, vol. 63, pp. 343–354, Jul. 2016, doi: 10.1016/j.isatra.2016.03.003.
- [18] I. Abzi, M. N. Kabbaj, and M. Benbrahim, "Robust Adaptive fractional-order sliding mode controller for vehicle longitudinal dynamic," in *2020 17th International Multi-Conference on Systems, Signals & Devices (SSD)*, Jul. 2020, pp. 1128–1132, doi: 10.1109/SSD49366.2020.9364239.
- [19] Y. Tang, X. Zhang, D. Zhang, G. Zhao, and X. Guan, "Fractional order sliding mode controller design for antilock braking systems," *Neurocomputing*, vol. 111, pp. 122–130, Jul. 2013, doi: 10.1016/j.neucom.2012.12.019.
- [20] Y. Tang, Y. Wang, M. Han, and Q. Lian, "Adaptive fuzzy fractional-order sliding mode controller design for antilock braking systems," *Journal of Dynamic Systems, Measurement, and Control*, vol. 138, no. 4, Apr. 2016, doi: 10.1115/1.4032555.
- [21] S. S. Moosapour, S. B. Fazeli Asl, and M. Azizi, "Adaptive fractional order fast terminal dynamic sliding mode controller design for antilock braking system (ABS)," *International Journal of Dynamics and Control*, vol. 7, no. 1, pp. 368–378, Mar. 2019, doi: 10.1007/s40435-018-0450-y.
- [22] M. Dousti, S. C. Baslamisli, E. T. Onder, and S. Solmaz, "Design of a multiple-model switching controller for ABS braking dynamics," *Transactions of the Institute of Measurement and Control*, vol. 37, no. 5, pp. 582–595, May 2015, doi: 10.1177/01422331214546522.
- [23] M. Burckhardt, *Fahrwerktechnik, radschlupf-regelsysteme*. Verlag: Vogel Business Media/VM, 1993.
- [24] A. Pati, S. Singh, and R. Negi, "Sliding mode controller design using PID sliding surface for half car suspension system," in *2014 Students Conference on Engineering and Systems*, May 2014, pp. 1–6, doi: 10.1109/SCES.2014.6880092.
- [25] T. Mizoshiri and Y. Mori, "Sliding mode control with a time-varying ellipsoidal sliding surface," in *2019 IEEE/SICE International Symposium on System Integration (SII)*, Jan. 2019, pp. 165–170, doi: 10.1109/SII.2019.8700396.
- [26] D. Matignon, "Stability properties for generalized fractional differential systems," *ESAIM: Proceedings*, vol. 5, pp. 145–158, Aug. 1998, doi: 10.1051/proc:1998004.

## BIOGRAPHIES OF AUTHORS






**Imane Abzi**    obtained the Engineer Degree in Mechatronics from Faculty of Sciences and Technologies of FEZ, Morocco in 2016. Since 2017, she has been working toward the Ph.D. degree at Engineering, Modeling and Systems Analysis Laboratory, USMBA, Fez, Morocco. She is the author of a paper published in the MDPI Journal Actuators under the Doi <https://doi.org/10.3390/act9040120>. Her research interests automotive engineering, robust and fault-tolerant control (FTC) of vehicle dynamics. She can be contacted at email: imane.abzi@usmba.ac.ma.



**Mohammed Nabil Kabbaj**    obtained two M.Sc. from UCL Belgium in 1999 and from UPS France in 2000 and his PhD from the University of Perpignan in 2004. He is a professor at Faculty of Sciences of Fez. His research interests include control and their engineering applications. He can be contacted at email n.kabbaj@usmba.ac.ma.



**Mohammed Benbrahim**    received his Engineering diploma from ENIM Rabat in 1997, and his M.Sc. and PhD degrees from EMI Rabat, in 2000 and 2007, respectively. He is a professor at Faculty of Sciences of Fez. His research interests include control and their engineering applications. He can be contacted at mohammed.benbrahim@usmba.ac.ma.